Journal of Solid State Chemistry 184 (2011) 2333–2338

Contents lists available at ScienceDirect

Journal of Solid State Chemistry

journal homepage: www.elsevier.com/locate/jssc

Crystallographic and magnetic properties of $(Cu_{1-x}V_x)V_2S_4$ ($x \approx 0.3$) single crystals with the layered defect NiAs structure synthesized under high pressure

Y. Klein [a,*], H. Moutaabbid [a], A. Soyer [a], M. D'Astuto [a], G. Rousse [a], J. Vigneron [b], A. Etcheberry [b], A. Gauzzi [a]

[a] Institut de Minéralogie et Physique des Milieux Condensés, Université Pierre et Marie Curie, CNRS UMR 7590, Campus Jussieu, 4 place Jussieu 75005 Paris, France
[b] Institut Lavoisier Versailles, Université de Versailles Saint-Quentin, CNRS UMR 8180, Bâtiment Lavoisier, 45 avenue des Etats-Unis 78035 Versailles Cedex, France

ARTICLE INFO

Article history:
Received 20 April 2011
Received in revised form
22 June 2011
Accepted 26 June 2011
Available online 2 July 2011

Keywords:
Transition metal sulfide
Defect NiAs structure
Single crystal
Magnetic susceptibility

ABSTRACT

We report on the reproducible growth of $(Cu_{1-x}V_x)V_2S_4$ single crystals of sizable dimensions ($\sim$0.3 mm) and homogeneous composition ($x \approx 0.3$) by means of high-pressure synthesis. The refinement of single crystal X-ray diffraction data indicates that the crystal structure is of the monoclinic defect NiAs-type, which consists of a stacking of VS_2 layers with CdI_2-type structure and chains of edge-sharing $(Cu_{1-x}V_x)S_6$ octahedra. Layers and chains form a network of face-sharing octahedra with no Cu–V intra-chain ordering. A combined X-ray photoelectron spectroscopy and bond valence sum analysis indicates that the valence of the V and Cu ions are 3+ and 1+, respectively. Magnetic susceptibility measurements unveil the coexistence of a large Pauli-like and of a small Curie-like paramagnetic contributions, with no evidence of any long range order down to 2 K. This result suggests a picture of predominantly itinerant 3*d* V electrons with significant electron–electron correlations.

1. Introduction

Structural phase transitions driven by pressure or temperature occur more frequently in transition metal sulfides than in their oxide counterparts owing to the amphoteric properties of sulfur and of the less ionic character of the chemical bonds in sulfides. As a result, chemical bonds in sulfides are more compressible, which favors changes of atomic coordination of the transition metals. These changes typically alter the width of the electronic bands and even the topology of the electronic structure. This point is illustrated by comparing the family of oxyspinels MM'_2O_4 with its sulfospinel counterpart MM'_2S_4 (*M*, *M'* transition metals) which crystallize in the cubic space group $Fd\bar{3}m$. While the former compounds generally are antiferromagnetic semiconductors, the latter ones exhibit a wide range of physical properties. In the M=Cu family, $CuIr_2S_4$ undergoes a metal–insulator transition at $T_{MI} \approx 226$ K [1,2], $CuRh_2S_4$ is superconducting with $T_C \approx 4.8$ K [3], $CuCr_2S_4$ is ferromagnetic with $T_C \approx 420$ K [4,5] and CuV_2S_4 displays a charge density wave (CDW) transition responsible of two sharp anomalies in the magnetic and transport properties at 55 and 90 K, respectively [6].

Such diversity of properties is enhanced by the polymorphism of sulfospinels MM'_2S_4, which may adopt an alternative monoclinic defect NiAs-type structure (space group $C2/m$) in addition to the above spinel structure. The stability of these two competing structures depends on the size and electronic configuration of the two *M* and *M'* metals [7–9]. As shown in Fig. 1, the alternative structure consists of a stacking of pseudo-hexagonal $M'S_2$ layers with a distorted CdI_2-type structure alternated with chains of edge-sharing MS_6 octahedra. This structure can also be described as a stacking of MS_2 and $M'S_2$ layers where half of the *M* sites are unoccupied, which forms empty channels along the *b*-axis. A variety of interesting physical phenomena have been observed in MM'_2S_4 compounds with defect NiAs-type structure, such as magnetic orderings in FeV_2S_4 [10], $NiCr_2S_4$ [11], and AMo_2S_4 (A=Fe or Co) [12], a first-order metal-metal transition in NiV_2S_4 [13], and a spin-glass behavior in $V_xCr_{3-x}S_4$ ($0.4 \le x \le 1$) [14]. In CuV_2S_4, the structural transition from spinel- to defect NiAs-type occurs at high temperature or pressure and the latter phase can be stabilized upon quenching from high temperature [8]. While the spinel phase of CuV_2S_4 has been widely studied, little is known about the defect NiAs-type phase, as only polycrystalline samples have been synthesized. The unit cell parameters are the only structural data available [8] and no physical property data have been hitherto reported. It is the aim of this paper to explore the stability conditions of the defect NiAs-type phase of $(Cu_{1-x}V_x)V_2S_4$ under

* Corresponding author. Fax: +33 1 4427 3785.
E-mail address: yannick.klein@impmc.upmc.fr (Y. Klein).

0022-4596/$ - see front matter © 2011 Elsevier Inc. All rights reserved.
doi:10.1016/j.jssc.2011.06.034

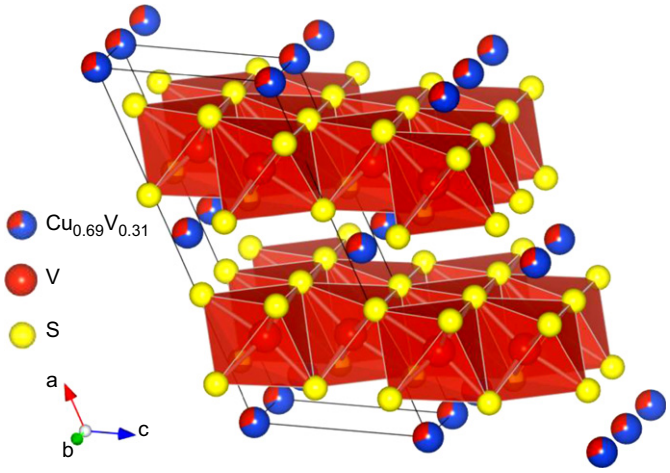

Fig. 1. Crystallographic structure of $(Cu_{0.69}V_{0.31})V_2S_4$. For clarity, the octahedral environment of $(Cu_{0.69}V_{0.31})$ site is not shown.

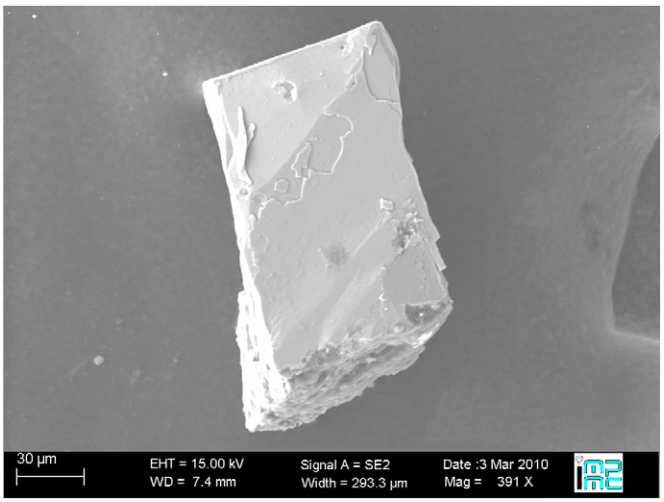

Fig. 2. A typical crystal that has been used for single crystal X-ray diffraction.

high pressure and to study the structural and magnetic properties of single crystals for $x \approx 0.3$. Our study is motivated by the possibility of electronic doping of the VS_2 layers through heterovalent substitutions at the Cu site, which may lead to electronic phase transitions.

2. Experimental

The title compound was obtained by studying the quaternary phase diagram Ca–Cu–V–S. Powders of CaS (Sigma, 99.9%), copper metal (Alfa Aesar, 99%), vanadium metal (Cerac, 99.7%) and pure sulfur (Sigma, 99.98%) were intimately mixed in a ratio of 1:3:4:11 and finely grounded in an agate mortar. The powders were then loaded in a 3.2 mm cell for high-pressure synthesis using a Paris-Edinburg VX3 hydraulic press, as described in detail elsewhere [15,16]. The powders were kept at 1000–1600 °C under quasi-hydrostatic conditions of 4–6 GPa during a time ranging from 1.5 to 20 h. The sample was subsequently quenched to room temperature by keeping the pressure constant. Note that the heated volume is very small ($\sim$100 mm^3) and the anvils are cooled by a system of water circulation, thus the quenching to room temperature is practically instantaneous. After the quenching, pressure was slowly released at a rate of 0.5 GPa/h.

The as-prepared samples consist of a mixture of black-turquoise single crystals and mixed with gray-colored polycrystalline powder. X-ray diffraction indicates that this powder is formed by CaS and various copper sulfides, such as CuS and CuS_2. Several single crystals could be easily selected from the powder matrix and observed by means of polarized optical microscopy. The best crystals with fairly regular parallelepedic shape and $0.6 \times 0.2 \times 0.2$ mm^3 size were reproducibly obtained after 1.5 h synthesis at 1300 °C and 4 GPa.

The temperature-dependent dc magnetization (M) of the crystals in the 2–300K range was measured using a commercial Quantum Design Magnetic Property Measurement System (MPMS) equipped with a 5 T superconducting magnet. In order to enhance the signal intensity, about 30 crystals of the same batch – corresponding to a mass of 2.6 mg – were positioned with the *ab*-planes parallel to the magnetic field on the sample holder using a small amount of N-type Apiezon grease. The contribution of the sample holder and grease were measured independently and subtracted from raw data. Both zero-field-cooling (ZFC) and field-cooling (FC) measurements were performed in a longitudinal field ranging from 100 to 3000 oersted.

The crystal structure was studied on a representative $0.15 \times 0.08 \times 0.03$ mm^3 single crystal (Fig. 2) by means of single crystal X-ray diffraction (XRD) using a commercial Oxford Xcalibur-S diffractometer (50 kV, 50 mA) equipped with a Mo $K\alpha$ radiation (λ=0.71069 Å) and a four-circle goniometer. The CrysAlis software [17] was employed for the control of the diffractometer and for data collection and analysis. The crystal structure was solved and refined using the SIR2004 and Crystals programs, respectively [18,19]. The microstructure and composition of a dozen crystals grown under the same conditions were studied by means of a commercial Field Emission Scanning Electron Microscope (Ultra 55 Zeiss) operated at 15 kV equipped with an energy dispersive spectroscopy (EDS) Bruker AXS 125 eV.

In order to determine the formal valence states of V, Cu and S, we carried out a systematic X-ray Photoelectron Spectroscopy (XPS) study on a representative crystal using a commercial XPS K-Alpha system (Thermo) equipped with an Al $K\alpha$ (1486.5 eV) X-ray monochromatized source with a band pass of 50 eV and an energy resolution of 0.6 eV. Typical base pressure in the vacuum chamber during the measurements was 5×10^{-10} Torr or better. The crystal samples were positioned on indium foils to ensure a good thermal and electrical contact with the sample holder. Binding energies were calibrated using a gold single crystal. The spot size of the X-ray beam impinging the sample surface was 50 µm.

Ambient temperature energy scans were performed to analyze the Cu 2*p*, S 2*p* and V 2*p* levels. Considering the photon energy (1486.5 eV) and the average binding energies (BE) of these levels, the mean escape depth, λ, of the photoelectrons is estimated to be 10 Å for Cu 2*p* line and 20 Å for S 2*p* and V 2*p* lines [20]. Therefore, considering that 95% of the total intensity originates from a layer of thickness 3λ, we conclude that the thickness of the layer probed in our measurement, is 6–7 times the distance between adjacent VS_2 layers and our XPS spectra is expected to reasonably reflect the bulk properties.

3. Results and discussion

The scanning electron micrograph of a representative sample is shown in Fig. 2. To verify the reliability of the EDS analysis, this analysis has been performed on a dozen single crystals and in about ten different spots on the surface for each crystal. For each crystal, the largest standard deviations from the average concentrations were 1%, 2% and 3% for Cu, V and S, respectively, but typical values

were much less, which shows the homogeneity of the crystals. The analysis also indicates that the majority of the samples exhibit the following ratios [Cu]/[S]$\sim 0.19 \pm 0.03$ and [V]/[S]$\sim 0.55 \pm 0.03$, which shows the compositional homogeneity of crystals of the same batch and the reproducibility of the results from run to run. No traces of calcium were found in any crystal. On the other hand, all synthesis carried out without using CaS as precursor yielded a mixture of polycrystalline powders and no trace of single crystals. This result suggests that CaS should play a role as a catalyst in the single crystal growth. This possibility is supported by our previous observation that CaS is found in the powder matrix.

Table 1
Crystal data and conditions of data collection.

Crystallographic data	
Symmetry	Monoclinic (*C*2/*m*, No. 12)
Cell parameters	$a=12.756(3)$ Å, $b=3.2933(6)$ Å, $c=5.8344(14)$ Å $\beta=116.06(3)^\circ$
V (Å^3)	220.2(1)
Z	2
Calculated density (g cm^{-3})	4.371
Data collection ($T=293$ K)	
Crystal size (mm^3)	Approx. $0.15 \times 0.08 \times 0.03$
Source of radiation	Mo $K\alpha$ with graphite monochromator
Diffractometer	Oxford Xcalibur S diffractometer
Detector	KM4CCD/Sapphire
Frames acquired	2133 (in 21 scans)
Scan step size (deg.)	1
Measured reflexions	2677
Max h, k, l	16, 4, 7
Absorption coefficient (mm^{-1})	9.804
Structure solution	
Programs used	Crysalis Pro (Oxford, Data processing) SIR2004 (structure solution) Crystals (refinement)
Reflexion used in the refinement	286
No. of refined parameters	22
Largest diff. peak and hole (e Å^{-3})	3.65
Reliability factor R	0.0515 ($I>3\sigma(I)$)
Weighted reliability factor wR	0.0567 ($I>3\sigma(I)$)

The indexing of the single-crystal X-ray diffraction spots unambiguously suggests a monoclinic *C*2/*m* space group with lattice parameters $a=12.756(3)$ Å, $b=3.2933(6)$ Å, $c=5.8344(14)$ Å, and $\beta=116.06(3)^\circ$, as shown in Table 1. Using the results of the above EDS analysis, the crystal structure could be successfully solved in a straightforward manner using the SIR2004 software. The refined structural parameters are reported in Table 2. We first considered a simple structural model corresponding to the CuV_2S_4 composition (see Fig. 1), where the V ions occupy the fourfold 4*i* layer site, the Cu ions occupy the twofold 2*a* chain site and the S atoms occupy two distinct 4*i* sites. The structural refinement using this model yielded a residual factor, $R=5.7\%$ with an anomalously high value for the thermal factor U of the Cu site. We explained this anomaly in terms of an excess of electron density on this site. A modified model with a Cu lacunar site, i.e. $Cu_{1-x}\square_xV_2S_4$ did improve the quality of the refinement but did not match the Cu/V cation ratio measured by EDS. We therefore refined the occupancy of this site by assuming a partial substitution of Cu for V. This model yielded a good quality refinement with $R=5.2\%$. The refinement indicates a partial substitution level of 30% for the chain site, in agreement with the EDS results. In order to increase the reliability of the refinement, an isotropic thermal factor was refined for this site, whilst the anisotropic thermal factors were refined for the other sites occupied by only one atom type. Indeed, for these sites, the refinement of the occupancy factors did not lead to any significant deviation from stoichiometry, so these factors were kept fixed. This result supports a previous report suggesting the preferential site occupancy of the M and M' cations in the MM'_2S_4 structure when the difference in atomic numbers of the two cations is sufficiently large [21]. According to this report, the light (heavy) cation V (Cu) tends to occupy the CdI_2-type layer (chain) site, respectively. The structural parameters of the refined structure and selected bond lengths are reported in Tables 2 and 3. Note the VS_2 layers in the *bc*-plane with a distorted CdI_2-type structure, which consists of an edge-sharing network of VS_6 octahedra. The Cu/V site also has an octahedral coordination and form chains of edge-sharing octahedra running between adjacent VS_2 layers. Contrary to the case of the binary compound VS_2, where the V–V bond distances take a unique value of 3.221 Å [22], in our case the VS_2 layers are strongly

Table 2
Atomic positions and thermal displacement parameters (Å^2).

Atom	Site	x	y	z	Occ
Cu(1)	2*a*	0	0	0	0.69(6)
V(1)	2*a*	0	0	0	0.31(6)
V(2)	4*i*	0.74483(11)	0	0.7060(3)	1
S(1)	4*i*	0.36053(17)	0	0.0248(3)	1
S(2)	4*i*	0.11617(17)	0	0.4550(4)	1

Atom	U_{iso} or U^*_{eq}	U_{11}	U_{22}	U_{33}	U_{12}	U_{13}	U_{23}
Cu(1)	0.035(5)	–	–	–	–	–	–
V(1)	0.012(10)	–	–	–	–	–	–
V(2)	0.0201	0.0241(8)	0.0150(7)	0.0232(8)	0	0.0122(6)	0
S(1)	0.0185	0.0267(10)	0.0111(9)	0.0191(9)	0	0.0115(7)	0
S(2)	0.0187	0.0260(10)	0.0112(9)	0.0207(9)	0	0.0118(7)	0

*U_{eq} is defined as one third of the trace of the orthogonalized U_{ij} tensor

Table 3
Selected interatomic distances (Å).

Cu(1)–S(1)	(×4)	2.475(2)	V(2)–S(1)	(×2)	2.437(2)	V(2)–V(2)	(×2)	3.293(1)
Cu(1)–S(2)	(×2)	2.406(2)	V(2)–S(1)		2.475(3)	V(2)–V(2)	(×2)	3.755(2)
Cu(1)–Cu(1)	(×2)	3.293(1)	V(2)–S(2)	(×2)	2.332(2)	V(2)–V(2)	(×2)	2.964(2)
Cu(1)–V(2)	(×2)	2.938(1)	V(2)–S(2)		2.343(2)			

distorted with two short, two intermediate and two long V–V bond distances with values of 2.965, 3.293, and 3.755 Å, respectively. The structure of the VS_2 layers is the same as in other members of the MM'_2S_4 family where zig-zag chains of cations are directed along the *b*-axis, breaking the 2D symmetry for a quasi-1D symmetry [23]. These distortions are explained by the presence of the uniaxial strain exerted by the adjacent chains of CuS_6 octahedra. A bond valence sum (BVS) analysis yields valence states of +1.13 for Cu(1) and +2.81 for V(1) in the chains, +3.32 for V(2) in the VS_2 layers, and −2.08 and −2.24 for S(1) and S(2), respectively. These values are supported by our XPS study summarized in Fig. 3a–c. A preliminary energy scan over a wide range indicates, as usual, the presence of CO_2 contamination at the surface and no evidence of surface oxidization. The first spectrum (see Fig. 3a) shows the detail of the Cu 2*p* doublet. For the $2p_{3/2}$ level, we find a binding energy (BE) of 932.7 eV attributed to the Cu^+ state, considering that the BE of standard Cu_2S and CuS samples is 932.0 and 931.4 eV, respectively [24,25]. This conclusion is supported by the absence of any shake-up satellite peak characteristic of the $3d^9$ ground state of the Cu^{2+} ion. This feature is found in the XPS spectra of CuO and CuS [25,26], where this ground state is indeed expected. We conclude that our data are rather consistent with the d^{10} ground state characteristic of Cu^+. Second, we consider the XPS spectra of the V 2*p* doublet shown in Fig. 3c. The $2p_{1/2}$ and $2p_{3/2}$ peak positions are at 520.3 and 512.4 eV, respectively. These values are to be compared with the $2p_{3/2}$ peak positions at 513.9 eV in VS [27], 512.6 eV in VP [28] and 514.4 eV in VN [29]. Note that V is divalent in the former compound and trivalent in VP and VN; the different peak positions in these two isoelectronic compounds reflects the different electronegativity of the trivalent N and P anions. Considering that the Pauling electronegativity of S is very close to that of P, we conclude that the dominant contribution to our spectra arises from the V^{3+} state, in agreement with the previous BVS analysis. The shoulder in both peaks of the doublet at the high binding energy side suggests a minor contribution of a higher valence state.

In Fig. 3b, we consider the XPS spectrum of the S 2*p* peak. This appears as a single broad peak due to the modest spin-orbit splitting of ~1.2 eV into $2p_{3/2}$ and $2p_{1/2}$ lines [30] convoluted with the instrumental broadening of 0.6 eV. The peak was fitted by a double Gaussian function with the same broadening for the two lines. The fit yields BE values of 162.2 and 163.5 eV for the $2p_{3/2}$ and $2p_{1/2}$ lines, respectively, and a broadening of 0.85 eV. A comparison with standard MgS, SrS, CaS and Na_2S spectra indicates that our BE values are consistent with a dominant contribution of the S^{2-} state [27,30]. The extra line broadening as compared to the instrumental broadening is attributed to the presence of two distinct *S* sites, *S*(1) and *S*(2), in the unit cell (see Table 2) as the valence of the S ion in these two sites is expected to be different. Specifically, the *S*(1) ions are more weakly bonded to the Cu or V ions, as indicated by the comparatively long five *S*(1)–*M* bonds in the 2.43–2.47 Å range (see Table 3). Opposite situation occurs for the *S*(2) ions, as the values of the four *S*(2)–*M* bond lenght fall in the 2.33–2.40 Å range.

Fig. 4 shows the magnetic susceptibility curve, $\chi(T)$, as a function of temperature. The data show that $Cu_{0.7}V_{2.3}S_4$ does not exhibit any magnetic long range order down to 2 K. No hysteresis was found by comparing the FC curve and the ZFC curve, which indicates the absence of other short range magnetic interactions characteristic of spin-glass systems. The curve is described by a

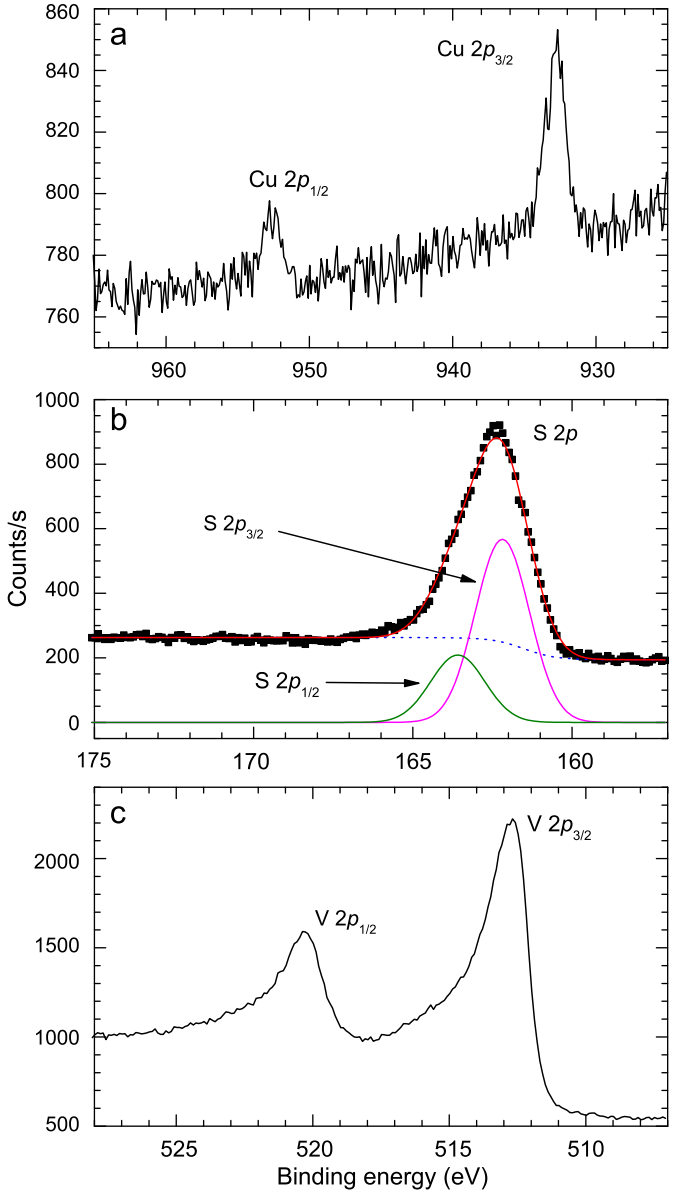

Fig. 3. XP spectra of the (a) Cu 2*p*, (b) S 2*p*, and (c) V 2*p* regions. For graph (b), black squares represent experimental data, blue dotted line background, green and purple lines $2p_{1/2}$ and $2p_{3/2}$ fitted functions, and red line total data fitting. (For interpretation of the references to color in this figure legend, the reader is referred to the web version of this article.)

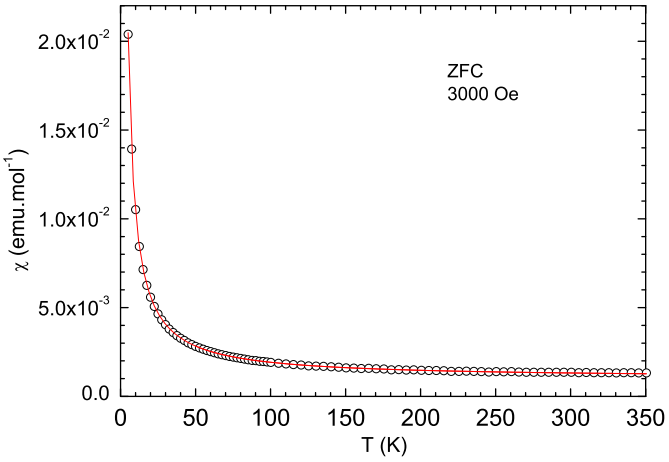

Fig. 4. Magnetic susceptibility of $Cu_{0.7}V_{2.3}S_4$ as a function of temperature, $\chi(T)$. Data were collected in the zero field cooled mode under a magnetic field of 0.3 T. Dots represent experimental data while the line represents the fit to the modified Curie law, $\chi(T)=\chi_0+C/(T-\theta)$.

Table 4
Comparison of the parameters of the magnetic susceptibility for MV_2S_4.

	M i	V	Cr	Fe	Ni	$Cu_{0.7}V_{0.3}$	Mo
χ_0 (10^{-3} emu mol^{-1})	1.69	1.34	3.22	1.53	1.21	1.02	1.15
C (emu K mol^{-1})	0.0442	0.020	0.253	1.11	0.019	0.090	0.016
θ (K)	−2.9	−4	−2.6	−108	−33	0	−17
μ_{eff}	0.18	0.43	1.42	2.98	0.39	0.72	0.35
Ref.	[21]	[31]	[21]	[21]	[21]	This work	[23]

Curie-Weiss law including a temperature-independent term, χ_0:

$$\chi = \chi_o + C/(T-\theta) \quad (1)$$

where $C = N_A\mu_{eff}^2\mu_B^2/3k_B$ and θ are the Curie and Weiss constants, respectively, k_B is the Boltzmann constant and μ_{eff} and μ_B indicate the effective moment and the Bohr magneton. The fitting yields $\mu_{eff}=0.72$, $\chi_0=1.02\times10^{-3}$ emu mol^{-1} and a negligible θ. In order to provide an account of these results we first note that, within a purely ionic model of Cu^{1+} ($S=0$) and V^{3+} ($S=1$), the expected μ_{eff} value is $\sqrt{2.3\times\mu_{eff}^2(V^{3+})}\approx4.29$, i.e. much larger than the experimental value. This discrepancy indicates that an ionic model is not valid in our case and a (Pauli) contribution of itinerant carriers should be included into the χ_0 term, in agreement with previous reports on other MV_2S_4 (M=Ti, V, Cr, Fe, Ni or Mo) sulfides with the same defect NiAs-type structure [21,23,31]. In order to estimate this contribution, we recall that the χ_0 term can be written as

$$\chi_0 = \chi_{core} + \chi_{VV} + \chi_{Pauli} + \chi_{LP} \quad (2)$$

where χ_{core} is the diamagnetic contribution of core electrons, χ_{VV} is the Van–Vleck paramagnetic contribution, χ_{Pauli} is the contribution of the itinerant carriers, and χ_{LP} is the Landau-Peierls correction to the Pauli paramagnetism ($\chi_{LP}=-\chi_{Pauli}/3$). According to our previous analysis, V^{3+} is the dominant oxidation state, thus we estimate $\chi_{core}\sim-1.83\times10^{-4}$ emu mol^{-1} [32]. On the other hand, the $\chi_{VV}\sim10^{-6}$ emu mol^{-1} contribution can be safely neglected. Therefore, from Eq. (2), we obtain $\chi_{Pauli}\sim1.8\times10^{-3}$ emu mol^{-1}, which enables us to estimate the density of states (DOS) $D(\varepsilon_F)$ at the Fermi level within the frame of a free electron gas model according to the expression

$$\chi_{Pauli} = \mu_B^2 D(\varepsilon_F) \quad (3)$$

From this expression, we obtain $D(\varepsilon_F)\sim19$ states eV^{-1} per metallic cations, *i.e.* Cu or V, an unusually large value for a three dimensional gas of non-interacting electrons. This observation leads us to conclude that the majority of the charges are itinerant, consistently with the small μ_{eff} value, and that the effective mass of these charges is significantly enhanced by correlation effects. A scenario of itinerant correlated charges is consistent with similarly anomalous values of χ_0 and of μ_{eff} observed in isostructural and isoelectronic compounds. The similarity is striking in Table 4, where we compare the relevant χ_0, C, θ and μ_{eff} parameters for all MV_2S_4 compounds with the defect NiAs-type structure hitherto reported. A similar scenario was also found in a previous paper on the doping-induced metal-insulator transition in the misfit layered compound $La_{1.17-x}Sr_xVS_{3.17}$ [33]. This similarity should not be surprising considering that the latter compound also displays a layered structure with the same CdI_2-type VS_2 planes and comparable χ_0 values. Indeed, for this system as well a picture of itinerant correlated electrons was proposed to explain this transition [34].

4. Conclusion

In conclusion, using high pressure and high temperature synthesis, we have succeeded in the reproducible growth of sizable and homogeneous $(Cu_{1-x}V_x)V_2S_4$ single crystals of the defect NiAs-type structure with $x\approx0.3$. The crystal structure consists of a stacking of VS_2 planes intercalated with chains of $(Cu_{0.7}V_{0.3})S_6$ octahedra. No ordering of the Cu and V ions is observed in these chains. An X-ray photoemission study combined to a bond valence sum analysis suggests a non-magnetic Cu^+ state. This analysis also indicates a majority of V^{3+} ions in both sites, although the data do not enable to rule out the presence of a minority of V^{4+} and V^{2+} in the VS_2 planes and in the $(Cu_{0.7}V_{0.3})S_6$ chains, respectively. The magnetic response unveils a paramagnetic behavior in the whole 2–300 K range investigated, with no indication of any long range magnetic order. The response is dominated by a Pauli term attributed to an unusually large density of states for a normal metal, in addition to a Curie-like contribution with a small effective moment/ion. We give an account of these results by invoking a simple two-band model, where the majority of the electrons display an itinerant behavior, whilst a minority of them is paramagnetic impurities. The unusually large value of density of states suggests the existence of a significant mass enhancement due to electronic correlations.

A confirmation of this scenario awaits further experimental studies as well as *ab initio* calculations of the electronic structure. In order to study the properties of the itinerant carriers, we shall attempt to tune their concentration by varying the relative proportion of copper and vanadium in the chain site. This would also enable to elucidate the question of the interplay between charge density wave state and metallic–metallic transition proposed for the parent compound NiV_2S_4.

Acknowledgments

We thank Y. Le Godec, S. Klotz, I. Estève, and A. Sellam for technical support and fruitful discussions.

References

[1] S. Nagata, T. Hagino, Y. Seki, T. Bitoh, Physica B 194 (1994) 1077.
[2] S. Nagata, N. Matsumoto, Y. Kayo, F. Furubayashi, T. Matsumoto, J.P. Sanchez, P. Vullet, Phys. Rev. B 58 (1998) 6844.
[3] T. Hagino, Y. Seki, N. Wada, S. Tsuji, T. Shirane, K. Kumagai, S. Nagata, Phys. Rev. B 51 (1995) 12673.
[4] F.K. Lotgering, R.P. Van Stapele, J. Appl. Phys. 39 (1968) 417.
[5] F.J. DiSalvo, J.V. Waszczak, Phys. Rev. B 26 (1982) 2501.
[6] I. Naik, C.S. Yadav, A.K. Rastogi, Phys. Rev. B 75 (2007) 115122.
[7] S. Ohta, S. Anzai, J. Pys. Chem. Solids 38 (1977) 1209.
[8] R.E. Tressler, F.A. Hummel, V.S. Stubican, J. Am. Ceram. Soc. 51 (1968) 648.
[9] R.J. Bouchard, Mater. Res. Bull. 2 (1967) 459.
[10] A.V. Powell, C. Ritter, P. Vaqueiro, J. Solid State Chem. 144 (1999) 372.
[11] A.V. Powell, D.C. Colgan, C. Ritter, J. Solid State Chem. 134 (1997) 110.
[12] P. Vaqueiro, M.L. Kosidowski, A.V. Powell, Chem. Mater. 14 (2002) 1201.
[13] Y.K. Kuo, K.M. Sivakumar, J.Y. Lin, C.N. Kuo, C.S. Lue, J. Phys.: Condens. Matter 19 (2007) 219210.

[14] A.V. Powell, S. Oestreich, J. Mater. Chem. 6 (1996) 807.
[15] S. Klotz, G. Hamel, J. Frelat, High Pressure Res. 24 (2004) 219.
[16] J.M. Besson, R.J. Nelmes, G. Hamel, J.S. Loveday, G. Weill, S. Hull, Physica B 180 (1992) 907.
[17] Oxford Diffraction, CrysAlis PRO CCD and CrysAlis PRO RED, Oxford Diffraction Ltd, Yarnton, England, 2009.
[18] M.C. Burla, R. Caliandro, M. Camalli, B. Carrozzini, G.L. Cascarano, L. De Caro, C. Giacovazzo, G. Polidori, R. Spagna, J. Appl. Cryst. 38 (2005) 381.
[19] P.W. Betteridge, J.R. Carruthers, R.I. Cooper, K. Prout, D. Watkin, J. Appl. Cryst. 36 (2003) 1487.
[20] S. Hüfner, Photoelectron Spectroscopy, Springer-Verlag, Berlin, Germany, 1995.
[21] V. Powell, D.C. Colgan, P. Vaqueiro, J. Mater. Chem. 9 (1999) 485.
[22] G.A. Wiegers, Physica B+C 99 (1980) 191.
[23] A.V. Powell, A. McDowall, P. Vaqueiro, R.I. Smith, T. Ohtani, Y. Okuya, J. Mater. Chem. 14 (2004) 3051.
[24] J.C.W. Folmer, F. Jellinek, J. Less-Comm. Metals 76 (1980) 153.
[25] D.L. Perry, J.A. Taylor, J. Mater. Sci. Lett. 5 (1986) 384.
[26] J. Ghisen, L.H. Tjeng, J. van Elp, H. Eskes, J. Westerink, G.A. Sawatsky, M.T. Czyzyk, Phys. Rev. B 38 (1988) 11322.
[27] H.F. Franzen, M.X. Umana, J.R. McCreary, R.J. Thorn, J. Solid State Chem. 18 (1976) 363.
[28] C.E. Myers, H.F. Franzen, J.W. Anderegg, Inorg. Chem. 24, (1822 (1985).
[29] M. Romand, M. Roubin, Analusis 4 (1976) 309.
[30] B.J. Lindberg, K. Hamrin, G. Johansson, U. Gelius, A. Fahlman, C. Nordling, K. Siegbahn, Phys. Scr. 1 (1970) 286 and references therein.
[31] Y. Tazuke, T. Sato, Y. Miyako, J. Phys. Soc. Jpn. 51 (1982) 2131.
[32] K.H. Hellwege, A.M. Hellwege, Landort–Börnstein, Springer-Verlag, Berlin, Germany, Group II 8 (1976) 27.
[33] T. Nishiwaka, Y. Yasui, Y. Kobayashi, M. Sato, J. Phys. Soc. Jpn. 65 (1996) 2543.
[34] A. Ino, T. Okane, S.-I. Fujimori, A. Fujimori, T. Mizokawa, Y. Yasui, T. Nishikawa, M. Sato, Phys. Rev. B 69 (2004) 195116.